Clot Monitoring Through Electromechanical Analysis

Hamzeh Abu Qamar[#1], Khaled Mohammed[#2], Sami Meetani[#3], Rashed Alketbi[#4], and Mahmoud Al Ahmad[#*]

Dept. of Electrical and Communication Engineering, United Arab Emirates University, Al Ain 15551, UAE

Email: {202050889, 201950180, 201950081, 201901085, m.alahmad}@uaeu.ac.ae

Abstract—**According to the World Health Organization, 32% of all global deaths are due to cardiovascular diseases; among the major contributors to these deaths are coronary heart diseases and strokes. Blood coagulation monitoring, accumulation rate, localization and prediction call for multidisciplinary efforts, to develop proper tools and models to quantify the coagulation process, because it is a complex physiological process that is fatal if present in an individual's tissues. The development of non-invasive rapid detection techniques incorporating spatial-temporal models of thrombus formation will help in the assessment process and benefit the global community. This work proposed a novel approach to detect the existence of a blood clot inside a vessel utilizing piezoelectric sensors. Hydrodynamics and the blood viscoelasticity theory have been integrated with the piezoelectric sensing theory to propose a method to track blood flow. The current approach incorporates four identical piezoelectric sensors that produce corresponding voltage signals. Under a particular arrangement, the piezoelectric sensors will record the electrical voltages at certain points, which are a result of the induced mechanical stress inside the vessel. The developed model will allow us to determine the vessel radius and the velocity of the blood at different locations. In case there is a significant change in radius of the blood vessel or velocity of the blood flow, this should be an indication to the presence of a clot or plaque accumulation inside the vessel. The continuity equation states that, for an incompressible fluid, the flow rate is conserved – which means that our procedure will allow us to extract vessel resistance. The outlined system has great potential as a novel blood coagulation monitoring technique.**

I. Introduction

Blood clots are semi-solid masses of blood that can either accumulate and stop blood flow or break off and move to different parts of the body [1]. The blood flow in the human body maintains a naturally steady flow rate that varies from person to other. However, when it blocks for various reasons, most notably blood coagulation [2], it can lead to severe illnesses such as heart attacks, brain strokes, and in severe cases, death [3]. A few decades ago, physicians began using different methods to locate the blood clot; some of which are still used today [4]. Ideally, the detection of heart attacks requires doctor's regular physical exams, where these tests are costly and require high skilled workers to operate them and professionals to interrupt the results. Ultrasound is one technique that is mainly used to check the carotid arteries or legs for physiological changes in the human body [5]. The visualization of internal organs in a specific part of the human anatomy can be performed by magnetic resonance imaging (MRI) [6], while computed tomography (CT) can be applied to inspect organs for internal bleeding [7]. However, because these methods are expensive, require high-skilled professionals to operate and take a "stab in the dark" by relying on risky X-rays, scanning for blood coagulation is dangerous [8]. Several invasive and non-invasive technologies have lately been utilized lately to detect and treat blood coagulation [9]. Venous ultrasonography has become more popular due to its promising results in validating the presence of a blood clot in veins [10]. Moreover, sound waves produce images of human veins, while Doppler ultrasonography displays the blood flow [11]. Most pulmonary embolisms are caused by clot fragments that migrate through the veins to the lungs [12]. In some circumstances, the doctor may request a cerebral angiography or carotid ultrasonography to see if a blood clot in the neck has affected the brain [14]. Blood clots can create symptoms that mirror other medical conditions; therefore, for diagnosis, the patient is required to do additional testing.

As a result, accurately identifying blood clots is increasing the demand for advanced research and development [16]. Using minuscule amounts of blood, the miniaturized Hemoretractometer (mHRM) was developed to take accurate measurements of dynamic clot retraction forces in real time [17]. Dissipation and viscosity are important parameters in analyzing blood flow rate [18]. Andersson, M., et al. researched real-time measurements of blood coagulation density [19]. It can be obtained from the sensor's frequency response, which is carried out by the quartz crystal microbalance (QCM) [20]. Thus far, a myriad of clinical trials were conducted using sensor technology in the field of blood clot detection [21]. For an instance, the clot chip is a portable device that uses dielectric spectroscopy to analyze the patient's hemostasis using single-drop blood samples [22]. Advanced integrating sensors are used to prevent clots from forming and dislodging themselves into the patient's blood stream with ECMO (extracorporeal membrane oxygenation)

tubing [23]. The micro-optical sensor method detects blood clots in artificial circulating apparatuses such as blood pumps [24]. Specifically, the sensor consists of three light-emitting diodes (LEDs) that allow the emission spectrum to be absorbed and scattered by the blood cell. If a blood clot is present, some of the red blood cells (RBCs) within the clot will flow out while others will remain stuck [25].

Since modern science is ever-evolving, capital is being heavily invested into portable technologies [26], which can be used to self-monitor. As a wearable device, piezoelectric sensors rapidly becoming an important element of the pharmacogenomics industry. It can be used to collect data from the human body and track health changes [27]. They have been selected over other sensors due to their structure, accuracy, simple signal processing, and most importantly their inexpensiveness [28]. These traits allow the piezoelectric sensors to drive up demand for biomedical instruments as they are currently being used in heart attack prediction methods, and blood clot detection systems. The early-stage piezoelectric sensors employed in blood coagulation used the viscosity change identification method [29]. Moreover, multi-pillar piezoelectric sensors were used for deep vein sonothrombolysis treatment [30]. Other methods discussed the effect electrical properties, i.e., conductivity and permittivity of human whole blood and its different components with/without various additives at different temperatures [31,32].

The piezoelectric plate method provides real-time continuous vital sign monitoring as, it is wearable and motion-free. Blood pressure, the blood flow rate, and the coagulation of blood are calculated using the piezoelectric sensor's data, which indicates that this system does not necessarily interfere of a physician. However, to link the sensors' dynamic response, more correlation is needed. By vibrating ultrasonic waves, the piezoelectric vibrator tip method detects blood coagulation [33]. The main advantage of such a system is that it operates at high frequencies, low amplitudes, and low power levels. However, the vibrations will always include undesirable bending due to the tip's length and flexibility. Patients can self-evaluate when external testing, however, a physician must handle internal testing procedure. The vibrator generated vibration for different diameters; In particular, a 3 mm length and 1.5 mm OD vibration tip stimulated at 30 kHz, showed promising results [34]. The piezoelectric quartz crystal (PQC) sensor is used to figure out how long it takes for the blood to clot and recalcified. A PQC sensor cannot predict blood coagulation on its own; it must be integrated with a coagulometer to correlate the frequency and viscosity changes from the sensor. In this method, the blood coagulation time is calculated outside of the body. Hence, this method can be handled by a technician who is skilled in blood and plasma laboratories. 10 MHz crystals have been used as a cost-effective material [34]. Another technique that can be used is the piezoelectric acoustic beam method. The multi-pillar piezoelectric stack (MPPS) transducer was developed to treat thrombosis, a condition that occurs when a blood clot forms in a deep vein. The miniaturized transducer is characterized by measuring the electrical impedance and acoustic pressure. Then, tests were conducted in blood flow-like system. The MPPS transducer delivered a high-pressure output of ~1.5 MPa to a distance of approximately 2.2 wavelengths from the aperture [35].

This work contributes to the development of non-invasive rapid detection techniques, incorporating piezoelectric sensors and hydrodynamics theory, to detect the existence of a blood clot inside a vessel. Under a particular arrangement, the piezoelectric sensors will record the electrical voltage signals allowing the determination of the vessel radius and the velocity of the blood at different locations. After the details of the current approach theory and modelling, the experimental setup and measurements analysis are presented. The results are discussed and compared with the state of the art and the study is concluded.

II. Current Approach Using Piezoelectric Theory

Piezoelectric materials have the ability to generate an internal electric field when subjected to mechanical stress. The open circuit output voltage (V_{oc}) of a piezoelectric sensor of a thickness (T) produced by a mechanical stress (σ) is related by the piezoelectric voltage constant (g) [36]:

$$V_{oc} = g\sigma T \tag{1}$$

In the current approach, this mechanical stress is induced by the blood flowing inside the vessel, which can be approximated by:

$$\sigma = \frac{4\eta Q}{\pi r^3} \tag{2}$$

where η is the blood viscosity, Q is the blood flow rate inside the vessel, and r is the inner radius of the vessel. Substituting (2) in (1) and rearranging for Q yields:

$$Q = \frac{\pi r^3}{4g\eta T} V_{oc} \tag{3}$$

Blood viscosity and the piezoelectric constant are known parameters. The viscosity – a measure of how thick the liquid is – can be determined for an individual using conventional existing methods [37]. The piezoelectric voltage constant depends on the properties of the piezoelectric material and the direction of polarization [38]. To compute the flow rate, the inner radius should be determined first. Flow rate is the product of the cross-sectional area of the vessel ($A = \pi r^2$) and the velocity (v) of the fluid at any given point, i.e. [39]:

$$Q = Av = \pi r^2 v \tag{4}$$

Substituting (4) in (3) and solving for r produces:

$$r = \frac{4g\eta v T}{V_{oc}} \tag{5}$$

The velocity of the fluid can be extracted by using two adjacent piezoelectric sensors separated by distance (d) and measuring the phase shift or time delay (Δt) between the two output signals. Hence, v can be determined by dividing the travel distance over the time delay, mathematically:

$$v = d/\Delta t \tag{6}$$

The proposed system (as shown in Figure 1) is composed of two sets of identical piezoelectric pairs (Pair 1 and Pair 2) separated by distance x. Each pair consists of two adjacent piezoelectric discs with a distance d between them. The system can be attached to the vessel using proper tools. The flow rate will be affected by the clot accumulation or plaque build-up inside the vessel. The technique above will allow us to extract the vessel radius and the velocity at different locations. If there is an accumulation of plaque, there will be a change in radius and velocity. The amount of change can be correlated with the clot dimensions.

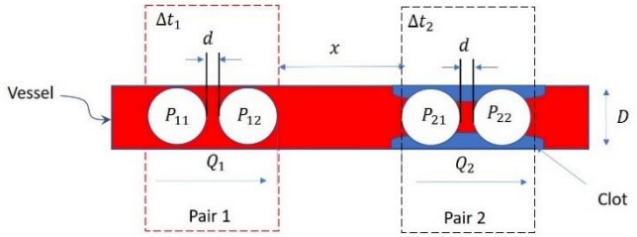

Fig. 1: Illustration of the proposed system overview

Furthermore, the continuity equation states that, for an incompressible fluid, the flow rate is conserved. The illustrated arrangement will also enable the extraction of vessel resistance (R) [39]:

$$R = \frac{\sigma_2 - \sigma_1}{Q} \tag{7}$$

where $\sigma_2 = (\sigma_{21} + \sigma_{22})/2$ and $\sigma_1 = (\sigma_{11} + \sigma_{12})/2$ are the average pressures of pair 2 and pair 1, respectively.

III. Measurements and Analysis

To demonstrate the power of the proposed approach, two piezoelectric desk sensors, each with diameter of 1cm, thickness of 0.125 mm and piezoelectric coefficient of 250 pm/V were employed. The designed experimental setup involves an oscilloscope, piezoelectric sensors, a tissue-like vessel, and a pump-system called the VI box. The VI box contains two separate 5V DC motors that pump aqueous solution into vessels, such as tissues. Two piezoelectric sensors are directly attached to two different points along the tissue-like vessel to measure the signals before and after the clot, as shown in Figure 2(a). As the aqueous solution flows through the vessel, the oscilloscope will display the signals – measured by the piezoelectric sensors – for data analysis. The prototype is used to figure out and predict the water flow rate and the rate of blockage buildup over time. For this reason, we need prototype models of human tissues as synthetic vessels, and a pump acting as a heart. Since the heart pumping rate is an important parameter, the similarity between the DC pump has been considered. Testing the blocked vessel with the pulse pumping motor is also considered as the pumping pulse rate may change due to the presence of a clot.

The VI box is employed in the commercialization of biomedical instrument prototype products. It includes various components such as synthetic vessels and tissues, a pump, and a power source. First, the pumping mechanism is required to circulate the liquid flow. The VI box consists of two color-coded pumps, which supply different rates of flow. To be specific, the blue pump provides a steady flow rate, while the red pump provides a pulsated flow with an irregular flow rate. The flow rate of aqueous solutions is calculated. By considering various parameters, which means that the flow may be disrupted if there are clots inside the vessel. As a result, the speed of the fluid flow can be determined by the cross-sectional area of the vessel, among other variables. In our experiment, we used prototype tissue-like vessels, with diameters ranging from 9 mm to 15 mm; some with clots in the middle to resemble plaque accumulation, as shown in Figure 2(b). For experimental comparison, aqueous solution was pumped, from the blue pump, first, and then, the red pump. We connected the piezoelectric sensors at opposite ends of the vessel tissue – specifically, before and after the clots for vessels with clot – and using the oscilloscope, we were able to record the signals. As a result, we collected data from the piezoelectric sensors in various-sized vessels with and without blockage for steady and unsteady water flow rates.

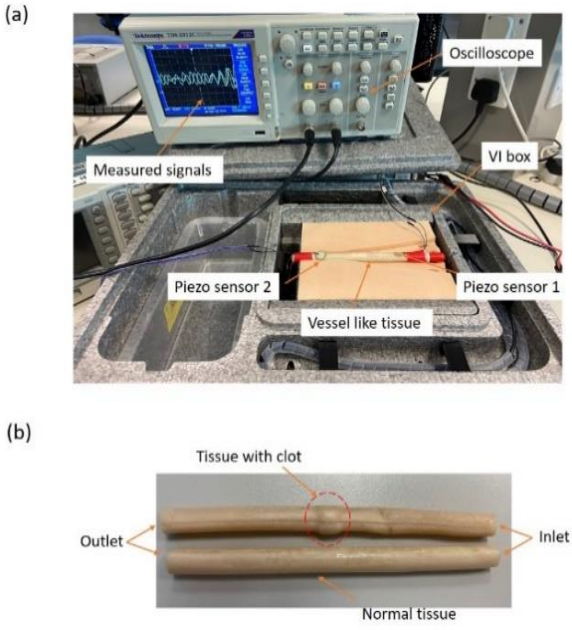

Fig. 2: Experimental setup of the prototype and display of the types of vessel-like tissues used

IV. Piezoelectric Sensor Characteristics

The piezoelectric transducer incorporated is a disc with diameter of 15 mm and thickness of 0.26 mm, composed of a lead-zirconate-titanate composition. Table I summarizes the material's most important properties.

Table 1
Properties of the Piezoelectric Sensor

Piezoelectric Properties	Symbol	Value and Unit
Dielectric constant	ε	4750
Dielectric loss	tan δ	25 x10^{-3}
Conductivity	σ_c	<1x10^{-12} 1/Ωm
Coercive field strength	E_c	570 x10^3 V/m
Piezoelectric voltage Constant	g	0.135 Vm/N
Piezoelectric charge Constant	d_{31} d_{33}	315 pm/V 640 pm/V

Two sets of available vessels with different diameters were employed in this study. Available in Small (5 mm ID), Medium (8.5 mm ID), and Large (10 mm ID), each vessel has a 1-1.25 mm wall thickness and comes in 6-inch lengths. One set without plaque and the second set a plaque were added to simulate atherosclerosis in vessels. The measure corresponding voltage signals are depicted in Figure3. Figure 3 illustrates the output voltages for the first set of uniform vessels with different diameters.

V. Materials and Methods

The VI Box, 0247 VI Embedded Veins with Dermis Model Veins embedded in soft tissue at different depths for vessel dissection and multiple end-to-end and end-to-side anastomosis training. 0204 Large Femoral Artery 6" Artery, 10 mm ID and 12.5 mm OD for basic end-to-end or end-to-side anastomosis training. 0235 Medium Femoral Artery 6" Artery, 8.5 mm ID and 11 mm OD for basic end-to-end or end-to-side anastomosis training. 0214 Small Femoral Artery 6" Artery, 5 mm ID and 7 mm OD for anastomosis training in the Femoral Leg Simulator, or to train basic end-to-end or end-to-side anastomosis from Life Like Bio Tissue Inc. [40].

VI. Results

Figure 3 depicts the measured output voltages of the piezoelectric sensor for different vessel diameters. As reflected in the figure, the output voltage signal increases with decreasing the vessel diameter. The induced stress on the vessel wall increases as its diameter decreases under constant water flow rate, in which these results prove and satisfy Eq. (2). In other words, having a clot means the radius of the vessel will decrease and cause increasing in the mechanical stress ($\boldsymbol{\sigma \propto \frac{1}{r^3}}$), in which this increasing in mechanical stress will be converted into a higher peak voltage. The measured voltage ranges approximately between -75 mV and +75 mV, which depend on the vessel diameter, liquid and piezoelectric sensor characteristics. The employed pump in this system has a frequency of 1 Hz and a maximum flow rate of 200 L/H; thus, the voltage profile exhibits a cycle of 1 second. The flow velocity decreases as vessel size increases. Using equations (3) and (5), considering the viscosity of water to be 1.0016 mPa.s at 20°C, and using the parameters in Table 2 for dimensions and piezoelectric sensor properties, the velocity of water, the acting stress on the vessel wall, and the induced stress on the piezoelectric sensor attached to the vessel were calculated for different vessel diameters (results were tabulated and displayed in Table 2.

Table 2
Velocity, acting stress, and induced stress for different vessel diameters.

Vessel Type	Length	Velocity	Acting Stress	Induced Stress	Extracted Radius
Units	(mm)	(m/s)	(10-7 Pa/mm2)	(kPa)	(mm)
Large	10	0.1769	0.0709	1.0709	0.4045
Medium	8.5	0.2448	0.0834	1.4993	0.3615
Small	5	0.7074	0.1417	1.7135	0.3458

Using equation (2), our focus now is to extract vessel radius directly from the measured sensor output voltage, given piezoelectric material parameters and dimensions. The actual radiuses were calculated and tabulated for further analysis in Table 2. Moreover, a calibration curve between the actual and extracted vessel radiuses was plotted in Figure 4.

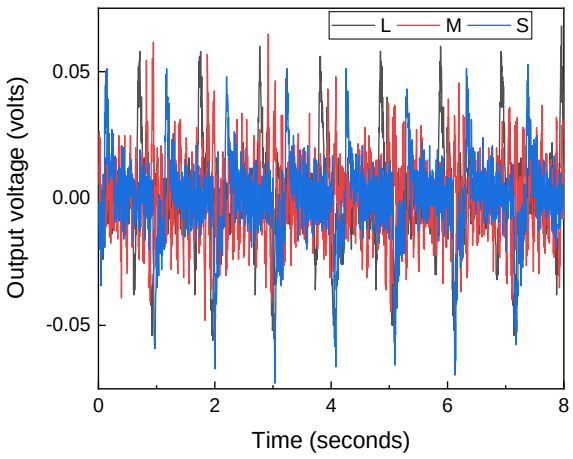

Fig. 3: Measured piezoelectric output voltages vs. time for different vessel

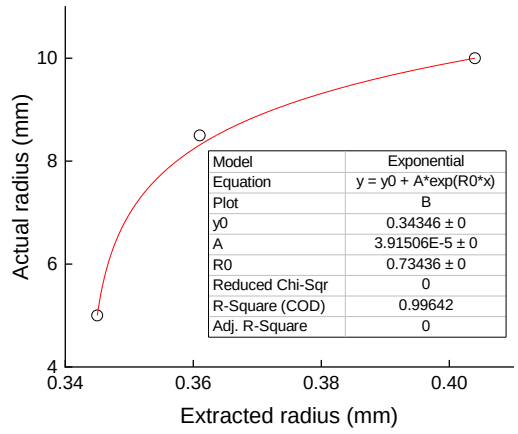

diameters: L, M, and S correspond to diameters 10 mm, 8.5 mm, and 5 mm, respectively.

Fig. 4: Calibration curve between actual radius and radius extracted from the sensor's measured output voltage.

Figure 5 depicts the measured sensor output voltages before and after the clot for one type of vessel. The voltage profile after the clot exhibits more noise in its signal, compared to the signal before the clot. As depicted the amplitude increased, and that periodicity disappeared; the signal before the clot has a fixed period of 1 sec, whereas that after the clot does not have a defined period. The presence of a clot in the vessel decreases the vessel radius, reducing the amount of water flow. With less water in the vessel, there will be more resonance in the tube, causing the output voltage to increase and the signal to spike. With this in mind, we can easily identify the presence of a clot by analyzing this sudden increase. The extracted radiuses for before and after the clot from the measured output voltages shown in Fig. 5 are found to be 0.49 mm and 0.385 mm, respectively (i.e., a 20% change).

Figure 6 shows the output voltage signal collected from a patient's wrist using the piezoelectric sensor as shown in Fig. 7. The corresponding measured blood pressures and the heartbeat rate for the test subject were 120/80 mmHg and 90 bpm. These values have been extracted using the method represented earlier [42]. The extracted signal period is equal to 0.7 seconds corresponding to a heartbeat of 85 bpm. The blood pressures extracted from the piezoelectric sensor are 123/82 mmHg. The computed effective pressure induced on the piezoelectric sensor is found to be 11.02 kPa, approximately equal to the measured diastolic blood pressure value. Accordingly, the extracted wrist vessel diameter is found to be 0.33 mm. The measured rest vein of the subject under test using ruler was approximately 2 mm. Therefore, according to Fig. 4, a correction factor should be introduced to account for this discrepancy, as done previously in the vessel. Therefore, the resistance of the blood vessel is calculated, using Eq. (7), and found to be 0.05 Pa.s/m3, inversely proportional to the radius of the blood vessel.

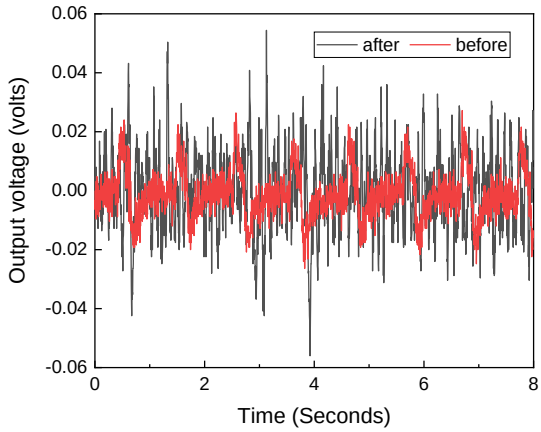

Fig. 5: Measured output voltage vs. time before and after the clot in the 10mm-diameter vessel.

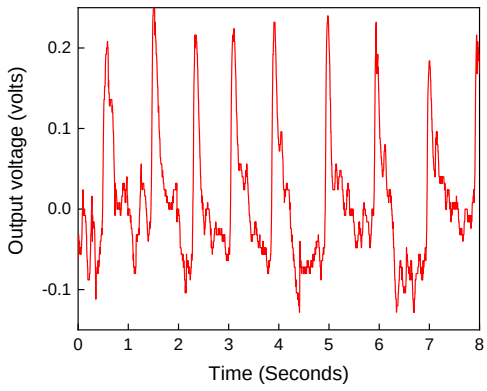

Fig. 6: Measured output voltage vs. time taken from a human's wrist.

VII. Conclusion

Based on its coupled electro-mechanically domains, the piezoelectric sensor was able to estimate the change in vessel radius and the velocity of the blood. In other words, the sensor was able to translate any change in the vessel diameter into a change in the corresponding measured electric signal. As a result, the extracted parameters will change, allowing us to predict the location of plaque accumulation in the arteries. The proposed system is inexpensive, efficient, and does not require physicians to operate or interpret results.

Acknowledgment

This work was supported by the United Arab Emirates University's Research Office, under the Summer Undergraduate Research Experience (SURE) 2022.

References

[1] S. R. Hanson, E. I. Tucker, and R. A. Latour, "Blood Coagulation and Blood–Material Interactions," in Biomaterials Science, Elsevier, 2020, pp. 801–812. doi: 10.1016/B978-0-12-816137-1.00052-0.

[2] M. J. Joyner and D. P. Casey, "Regulation of Increased Blood Flow (Hyperemia) to Muscles During Exercise: A Hierarchy of Competing Physiological Needs," Physiol. Rev., vol. 95, no. 2, pp. 549–601, Apr. 2015, doi: 10.1152/physrev.00035.2013.

[3] R. K. Jain and P. F. Carmeliet, "Vessels of Death or Life," Sci. Am., vol. 285, no. 6, pp. 38–45, Dec. 2001, doi: 10.1038/scientificamerican1201-38.

[4] P. A. Gentry, "Comparative aspects of blood coagulation," Vet. J., vol. 168, no. 3, pp. 238–251, Nov. 2004, doi: 10.1016/j.tvjl.2003.09.013.

[5] B.-M. Nguyen, K. W. Lin, and R. Mishori, "Public health implications of overscreening for carotid artery stenosis, prediabetes, and thyroid cancer," Public Health Rev., vol. 39, no. 1, p. 18, Dec. 2018, doi: 10.1186/s40985-018-0095-6.

[6] V. P. B. Grover, J. M. Tognarelli, M. M. E. Crossey, I. J. Cox, S. D. Taylor-Robinson, and M. J. W. McPhail, "Magnetic Resonance Imaging: Principles and Techniques: Lessons for Clinicians," J. Clin. Exp. Hepatol., vol. 5, no. 3, pp. 246–255, Sep. 2015, doi: 10.1016/j.jceh.2015.08.001.

[7] M. S. Lauer, "Elements of Danger — The Case of Medical Imaging," N. Engl. J. Med., vol. 361, no. 9, pp. 841–843, Aug. 2009, doi: 10.1056/NEJMp0904735.

[8] T. Bodnár and A. Sequeira, "Numerical Simulation of the Coagulation Dynamics of Blood," Comput. Math. Methods Med., vol. 9, no. 2, pp. 83–104, 2008, doi: 10.1080/17486700701852784.

[10] S. Zhang et al., "Evaluation of stability of deep venous thrombosis of the lower extremities using Doppler ultrasound," J. Int. Med. Res., vol. 48, no. 8, p. 030006052094209, Aug. 2020, doi: 10.1177/0300060520942098.

[11] A. Carovac, F. Smajlovic, and D. Junuzovic, "Application of Ultrasound in Medicine," Acta Inform. Medica, vol. 19, no. 3, p. 168, 2011, doi: 10.5455/aim.2011.19.168-171.

[12] M. L. Schiebler et al., "Effectiveness of MR angiography for the primary diagnosis of acute pulmonary embolism: Clinical outcomes at 3 months and 1 year," J. Magn. Reson. Imaging, vol. 38, no. 4, pp. 914–925, Oct. 2013, doi: 10.1002/jmri.24057.

[13] S. L. Mayne, K. A. Moore, T. M. Powell-Wiley, K. R. Evenson, R. Block, and K. N. Kershaw, "Longitudinal Associations of Neighborhood Crime and Perceived Safety With Blood Pressure: The Multi-Ethnic Study of Atherosclerosis (MESA)," Am. J. Hypertens., vol. 31, no. 9, pp. 1024–1032, Aug. 2018, doi: 10.1093/ajh/hpy066.

[14] M. Kishikawa, K., Kamouchi, M., Okada, Y., Inoue, T., Ibayashi, S., & Iida, "Evaluation of Distal Extracranial Internal Carotid Artery by Transoral Carotid Ultrasonography in Patients with Severe Carotid Stenosis," AJNR Am J Neuroradiol. 2002 Jun; 23(6) 924–928..

[16] A. Papadopoulou, H. Musa, M. Sivaganesan, D. McCoy, P. Deloukas, and E. Marouli, "COVID-19 susceptibility variants associate with blood clots, thrombophlebitis and circulatory diseases," PLoS One, vol. 16, no. 9, p. e0256988, Sep. 2021, doi: 10.1371/journal.pone.0256988.

[17] Z. Li, X. Li, B. McCracken, Y. Shao, K. Ward, and J. Fu, "Clot Retraction: A Miniaturized Hemoretractometer for Blood Clot Retraction Testing (Small 29/2016)," Small, vol. 12, no. 29, pp. 3925–3925, Aug. 2016, doi: 10.1002/smll.201670144.

[18] B. K. Sharma and C. Kumawat, "Impact of temperature dependent viscosity and thermal conductivity on MHD blood flow through a stretching surface with ohmic effect and chemical reaction," Nonlinear Eng., vol. 10, no. 1, pp. 255–271, Jan. 2021, doi: 10.1515/nleng-2021-0020.

[19] M. Andersson, J. Andersson, A. Sellborn, M. Berglin, B. Nilsson, and H. Elwing, "Quartz crystal microbalance-with dissipation monitoring (QCM-D) for real time measurements of blood coagulation density and immune complement activation on artificial surfaces," Biosens. Bioelectron., vol. 21, no. 1, pp. 79–86, Jul. 2005, doi: 10.1016/j.bios.2004.09.026.

[21] S.-H. Liu, J.-J. Wang, W. Chen, K.-L. Pan, and C.-H. Su, "An Examination System to Detect Deep Vein Thrombosis of a Lower Limb Using Light Reflection Rheography," Sensors, vol. 21, no. 7, p. 2446, Apr. 2021, doi: 10.3390/s21072446.

[22] D. Maji et al., "ClotChip: A Microfluidic Dielectric Sensor for Point-of-Care Assessment of Hemostasis," IEEE Trans. Biomed. Circuits Syst., vol. 11, no. 6, pp. 1459–1469, Dec. 2017, doi: 10.1109/TBCAS.2017.2739724.

[23] C. A. Figueroa Villalba, D. M. McMullan, R. C. Reed, and W. L. Chandler, "Thrombosis in Extracorporeal Membrane Oxygenation (ECMO) Circuits," ASAIO J., vol. 68, no. 8, pp. 1083–1092, Aug. 2022, doi: 10.1097/MAT.0000000000001605.

[24] N. Morita et al., "Real-time, non-invasive thrombus detection in an extracorporeal circuit using micro-optical thrombus sensors," Int. J. Artif. Organs, vol. 44, no. 8, pp. 565–573, Aug. 2021, doi: 10.1177/0391398820978656.

[25] C. Buzea, I. I. Pacheco, and K. Robbie, "Nanomaterials and nanoparticles: Sources and toxicity," Biointerphases, vol. 2, no. 4, pp. MR17–MR71, Dec. 2007, doi: 10.1116/1.2815690.

[26] Y. Xin et al., "Recent progress on the wearable devices based on piezoelectric sensors," Ferroelectrics, vol. 531, no. 1, pp. 102–113, Jul. 2018, doi: 10.1080/00150193.2018.1497411.

[27] Y. Yuan et al., "Highly sensitive and wearable bionic piezoelectric sensor for human respiratory monitoring," Sensors Actuators A Phys., vol. 345, p. 113818, Oct. 2022, doi: 10.1016/j.sna.2022.113818.

[28] Z. Yi et al., "Piezoelectric Dynamics of Arterial Pulse for Wearable Continuous Blood Pressure Monitoring," Adv. Mater., vol. 34, no. 16, p. 2110291, Apr. 2022, doi: 10.1002/adma.202110291.

[29] T. Li, J. Ma, S. D. Kumar, and A. F. Low, "Development of Piezoelectric Ultrasonic Thrombolysis Device for Blood Clot Emulsification," ISRN Mater. Sci., vol. 2012, pp. 1–6, May 2012, doi: 10.5402/2012/106484.

[30] H. Kim, J. Kim, H. Wu, B. Zhang, P. A. Dayton, and X. Jiang, "A multi-pillar piezoelectric stack transducer for nanodroplet mediated intravascular sonothrombolysis," Ultrasonics, vol. 116, p. 106520, Sep. 2021, doi: 10.1016/j.ultras.2021.106520.

[31] S. Kumari and S. K. Samanta, "The Effect of Temperature and Additives on the Dielectric Behavior of Human Whole Blood, Its Different Components, and Cell Suspensions," in IEEE Transactions on Instrumentation and Measurement, vol. 71, pp. 1-9, 2022, Art no. 1001809, doi: 10.1109/TIM.2022.3141078.

[32] Tzong-Jih Cheng, Hsein-Chang Chang, and Tsun-Mei Lin, "A piezoelectric quartz crystal sensor for the determination of coagulation time in plasma and whole blood," Biosens. Bioelectron., vol. 13, no. 2, pp. 147–156, Feb. 1998, doi: 10.1016/S0956-5663(97)00111-5.

[33] R. L. Bunde, E. J. Jarvi, and J. J. Rosentreter, "Piezoelectric quartz crystal biosensors," Talanta, vol. 46, no. 6, pp. 1223–1236, Aug. 1998, doi: 10.1016/S0039-9140(97)00392-5.

[34] Y. Zhou, D.J. Apo, M. Sanghadasa, M. Bichurin, V.M. Petrov, S. Priya, Magnetoelectric energy harvester, In Woodhead Publishing Series in Electronic and Optical Materials, Composite Magnetoelectrics, Woodhead

Publishing, 2015, Pages 161-207, ISBN 9781782422549,https://doi.org/10.1016/B978-1-78242-254-9.00007-X.
[35]Marvin RS. The Accuracy of Measurements of Viscosity of Liquids. J Res Natl Bur Stand A Phys Chem. 1971 Nov-Dec;75A(6):535-540. doi: 10.6028/jres.075A.041.
[36] N. Sezer and M. Koç, "A comprehensive review on the state-of-the-art of piezoelectric energy harvesting," *Nano Energy*, vol. 80, p. 105567, Feb. 2021, doi: 10.1016/j.nanoen.2020.105567.
[37]"Viscosity - Definition, meaning, types, formula, unit, example," *BYJUS*, Feb. 20, 2023. https://byjus.com/physics/viscosity/
[38]T.-B. Xu, "Energy harvesting using piezoelectric materials in aerospace structures," in *Elsevier eBooks*, 2016, pp. 175–212. doi: 10.1016/b978-0-08-100148-6.00007-x.
[39]Derivation of continuity equation - continuity equation derivation. BYJUS. (2022, December 13). https://byjus.com/physics/derivation-of-continuity-equation/
[40]Lifelike biotissue. LifeLike BioTissue. (n.d.). https://lifelikebiotissue.com/